Carbohydrate Polymers 94 (2013) 106–113

Contents lists available at SciVerse ScienceDirect

Carbohydrate Polymers

journal homepage: www.elsevier.com/locate/carbpol

Composite polyelectrolyte multilayer membranes for oligosaccharides nanofiltration separation

Jiafu Shi, Wenyan Zhang, Yanlei Su, Zhongyi Jiang*

Key Laboratory for Green Technology of Ministry of Education, School of Chemical Engineering and Technology, Tianjin University, Tianjin 300072, China

ARTICLE INFO

Article history:
Received 7 July 2012
Received in revised form
29 September 2012
Accepted 18 January 2013
Available online 25 January 2013

Keywords:
Oligosaccharides
Stepwise separation
Composite polyelectrolyte multilayer
Nanofiltration membrane
Layer-by-layer assembly

ABSTRACT

In the present work, composite polyelectrolyte multilayer (C-PEM) membranes were fabricated by using layer-by-layer (LbL) assembly technique for oligosaccharides nanofiltration (NF) separation. Specifically, the (chitosan/poly(styrene sulfonate) (PSS))$_3$ multilayers designated as the middle layer (ML) were first deposited on the hydrolyzed polyacrylonitrile (PAN) ultrafiltration membranes, which were designated as the support layer. Then, the (poly(allylamine hydrochloride) (PAH)/PSS)$_2$ multilayers designated as the top layer (TL) were deposited on the ML to form C-PEM membranes. When utilized for oligosaccharides NF separation, C-PEM membranes exhibited desirable performance compared to single-paired PEM membranes such as (PAH/PSS)$_5$ and (chitosan/PSS)$_5$ membranes owing to the collaboration of the TL and ML. In detail, C-PEM membranes acquired a permeation flux of 3.7 ± 0.3 Lm^{-2} h^{-1}, 100% rejection of oligosaccharides and 63.0 ± 0.5% rejection of glucose along with a high maltose/glucose selectivity of 46, demonstrating the promising potential for one-step membrane separation of oligosaccharides mixture.

1. Introduction

Nowadays, oligosaccharides have been widely utilized as food and feed ingredients or additives (Xu, Chao, & Wan, 2009) owing to their great healthcare and nutrition functions (*e.g.* bifidus-stimulating activity, low calorific value, low cariogenic property, *etc.*) (Mussatto & Mancilha, 2007). Generally, oligosaccharides were mainly produced *via* biochemical reactions. And oligosaccharides product in the reaction mixture often possessed a yield of lower than 50 *wt%*, containing high content of monosaccharides (*e.g.* glucose, galactose, *etc.*). For functional foods applications, oligosaccharides with low content of monosaccharides were considered to be the target products and highly desired (Anderson & Hanna, 1999; López-Leiva & Guzman, 1995; Roberfroid, 1999). Therefore, an efficient separation of oligosaccharides and monosaccharides was indispensable. Nanofiltration (NF) has been demonstrated as a feasible technology for the separation and purification of oligosaccharides (Feng, Chang, Wang, & Ma, 2009; Goulas, Grandison, & Rastall, 2003; Kamada, Nakajima, Nabetani, Saglam, & Iwamoto, 2002; Li, Li, Chen, & Chen, 2004; Zhao et al., 2012). However, previous efforts were mainly focused on utilizing commercial NF membranes for obtaining high purity of oligosaccharides product. Since these commercial membranes usually exhibited relatively low rejection of oligosaccharides, the feed solution must be recycled for a number of times to avoid the loss of oligosaccharides. Therefore, developing strategies for fabricating NF membranes displaying high rejection of oligosaccharides and high selectivity of oligosaccharides/monosaccharides has proven an urgent and challenging task.

Recently, layer-by-layer (LbL) assembly technique has developed rapidly as a facile and versatile surface modification technique for fabricating ultrathin polyelectrolyte multilayers (PEMs). Considering the merits of PEMs such as tunable pore size, ultrathin and controllable selective layer, facilitated mass transport, several research groups (Ahmadiannaminia et al., 2012; Jin, Toutianoush, & Tieke, 2003; Li et al., 2008; Miller & Bruening, 2004; Stanton, Harris, Miller, & Bruening, 2003) have exploited PEMs to fabricate NF membranes (Wang, Yao, Yue, & Economy, 2009). Till now, the application of PEMs in NF membrane fabrication was primarily focused on fabricating PEMs with only a single pair of polycation or polyanion such as poly(styrene sulfonate) (PSS)/poly(allylamine hydrochloride) (PAH) (PSS/PAH) (Stanton et al., 2003), PSS/poly (diallyldimethylammonium chloride) (PDDA) (Miller & Bruening, 2004), poly(vinyl amine)/poly(vinyl sulfate) (Jin et al., 2003) and sulfonated poly (ether ether ketone) (SPEEK)/PDDA (Li et al., 2008). These types of membranes usually exhibited desirable performance in rejection of one component or separation of binary mixture, but they might not well meet the requirements for separation of ternary mixture or mixture containing more than four kinds of components, especially for the mixtures with wide

* Corresponding author at: School of Chemical Engineering & Technology, Tianjin University, 92 Weijin Road, Nankai District, Tianjin 300072, China. Tel.: +86 22 2350 0086; fax: +86 22 2350 0086.
E-mail address: zhyjiang@tju.edu.cn (Z. Jiang).

0144-8617/$ – see front matter © 2013 Elsevier Ltd. All rights reserved.
http://dx.doi.org/10.1016/j.carbpol.2013.01.044

molecular weight range such as oligosaccharides mixture. For such a separation task, stepwise separation using a single sheet of membrane would be often expected.

In the present study, composite polyelectrolyte multilayer (C-PEM) membranes containing two different polyelectrolyte pairs as the active layer were prepared. Specifically, one pair was PAH/PSS, another pair was chitosan/PSS which was seldom utilized individually for fabricating PEMs due to the high hydrophilicity of chitosan (Beppu, Vieira, Aimoli, & Santana, 2007; Chen et al., 2008; De Oliveira, Fonseca, & Pereira, 2008). Hydrolyzed polyacrylonitrile (PAN) ultrafiltration membranes were selected as the support layer to ensure good adhesion. Isomaltooligosaccharides (IMO500) containing 41 *wt%* glucose, 27 *wt%* maltose and isomaltose (collectively called maltose hereafter) and 32 *wt%* oligosaccharides (trisaccharide and above) were chosen as the separation system. According to the literatures (Miller & Bruening, 2004; Richert et al., 2004) and our preliminary experiment, $(chitosan/PSS)_5$ membranes allowed an essentially complete passage of glucose with relatively high permeation flux and low rejection for oligosaccharides, while $(PAH/PSS)_5$ membranes displayed the opposite trend, possessing high rejection for glucose, maltose and oligosaccharides, but rather low permeation flux. Therefore, NF membranes with a unique structure were constructed for stepwise oligosaccharides separation. The $(chitosan/PSS)_3$ multilayers as the middle layer (ML) were firstly deposited on the support layer. Then, the $(PAH/PSS)_2$ multilayers as the top layer (TL) were deposited on the ML to form C-PEM membranes. The TL was served as the barrier for totally rejecting oligosaccharide and largely rejecting maltose, while the ML was mainly responsible for rejecting the residual maltose and passing the majority of glucose. Moreover, the chemical composition, structural morphology and NF performance of C-PEM membranes were detailedly characterized.

2. Material and methods

2.1. Materials

Polyacrylonitrile (PAN) powders were purchased from Shuguang Chemical Co. (Shanghai, China) and used without pretreatment. Chitosan with a degree of deacetylation of 90% was supplied from Zhejiang Golden-shell Biochemical Co. (Zhejiang, China). Dimethyl sulfoxide (DMSO), acetic acid and sodium chloride (NaCl) were obtained from Jiangtian Chemical Reagent Co. (Tianjin, China). Isomaltooligosaccharides (IMO500), that contained 41 *wt%* glucose, 27 *wt%* maltose and isomaltose (collectively called maltose hereafter) and 32 *wt%* oligosaccharides (trisaccharide and above), were supplied from Tianjun Co. (Tianjin, China). Polyethyleneimine (PEI, M_w = 25 kDa, 50 *wt%* aq.), poly(allylamine hydrochloride) (PAH, M_w = 70 kDa) and poly(styrene sulfonic acid) sodium salt (PSS, M_w = 70 kDa) were purchased from Sigma–Aldrich Chem. Co. Deionized water was used throughout all the experiments.

2.2. Preparation of the hydrolyzed asymmetric PAN ultrafiltration membranes

The asymmetric PAN membranes were fabricated *via* phase inversion technique with 14 *wt%* PAN powders dissolved in DMSO. The polymer solution was cast on a glass plate and then immersed in deionized water. Subsequently, the hydrolyzed PAN membranes were obtained by immersing the PAN membranes in 1.5 M NaOH (aq.) at 60 °C for 1 h. The residual NaOH was removed by rinsing with large amount of water. Before fabricating the polyelectrolyte multilayer (PEM) membranes, the hydrolyzed PAN membranes were first immersed in 3.6 *wt%* HCl for 0.5 h to convert–COO^- group into –COOH group.

2.3. Preparation of the PEM membranes

The hydrolyzed PAN membranes were completely soaked with water and then placed in a dead-end cell to ensure only one side of the membranes being exposed to the polyelectrolyte solutions. The fabrication of composite polyelectrolyte multilayer (C-PEM) membranes started with the immersion of the hydrolyzed PAN membranes in 2 gL^{-1} PEI solution (pH 9.0, 0.5 M NaCl, aq.) for 10 min and rinsed with deionized water for 1 min. Then, the PEI-treated membranes were immersed in 2 gL^{-1} PSS solution (pH 6.5, 0.5 M NaCl, aq.) for 10 min followed by rinsing with deionized water for 1 min. The middle layer (ML) which comprised three chitosan/PSS bilayers was constructed firstly with a 10 min immersion of the above substrate in 2 gL^{-1} chitosan solution (pH 4.5, 0.5 M NaCl, acetic acid aq.) and then rinsed with deionized water for 1 mine before a 10 min immersion in 2 gL^{-1} PSS solution. The as-synthesized membranes were then capped with two PAH/PSS bilayers (2 gL^{-1} PAH solution, pH 4.0, 0.5 M NaCl, aq.) to form the top layer (TL) following the same immersing and rinsing procedures.

For PAH/PSS or chitosan/PSS membranes, the hydrolyzed PAN membranes were only immersed in PAH/PSS solution or chitosan/PSS solutions. The deposition conditions (type and concentration of polyelectrolytes, pH value) and immersion time were chosen upon specific requirement (as shown in Fig. 1).

2.4. Characterizations

The surface and cross-sectional morphologies of the membranes were characterized by SEM (Philips XL-30 ESEM). ATR-FTIR spectra were measured in transmittance mode on a Nicolet, MAGNA-IR 560 instrument with a resolution of 4 cm^{-1}. The thickness of the PEMs for C-PEM membranes was obtained by AFM (AJ-III, Aijian nanotechnology Inc., China) measurement, which was carried out in air under normal conditions. Solution viscosity was measured by using Viscometer (DV-I Prime, Brookfield engineering laboratories Inc., USA). Considering the difficulty on measuring the surface zeta-potentials of C-PEM membranes as a function of layer number, PSS-doped $CaCO_3$ microspheres were utilized as the substrate instead of the hydrolyzed PAN membranes. The surface zeta-potentials of C-PEM microparticles as a function of layer number were measured in water by a Brookhaven zeta-potential analyzer.

2.5. Nanofiltration (NF) process

A dead-end stirred cell filtration system with a N_2 gas cylinder and solution reservoir connected was designed to testify the permeation flux of the membranes. The system consisted of a filtration cell (Model 8200, Millipore Co.) with a vertical-blade magnetic stirrer assembly. The impeller diameter (D) was about 49 mm and its distance to the membrane surface was set at about 40 mm during the filtration process. The volume capacity of the filtration cell was 200 mL and the inner diameter was about 62 mm. The effective area of the membranes was 28.7 cm^2. The feed side of the system was compressed by N_2 gas. After fixing the membranes, the stirred cell was filled with IMO500 aqueous solution. The solution permeation flux (J, $Lm^{-2}\,h^{-1}$) was then calculated by Eq. (1)

$$J = \frac{V}{A \times \Delta t} \tag{1}$$

where V was the volume of permeated solution (L), A was the membrane area (m^2), and Δt was the permeation time (h). Most of the NF experiments were carried out at a stirring speed of about 400 rpm, temperature of 25 ± 1 °C and operation pressure of 0.3 MPa.

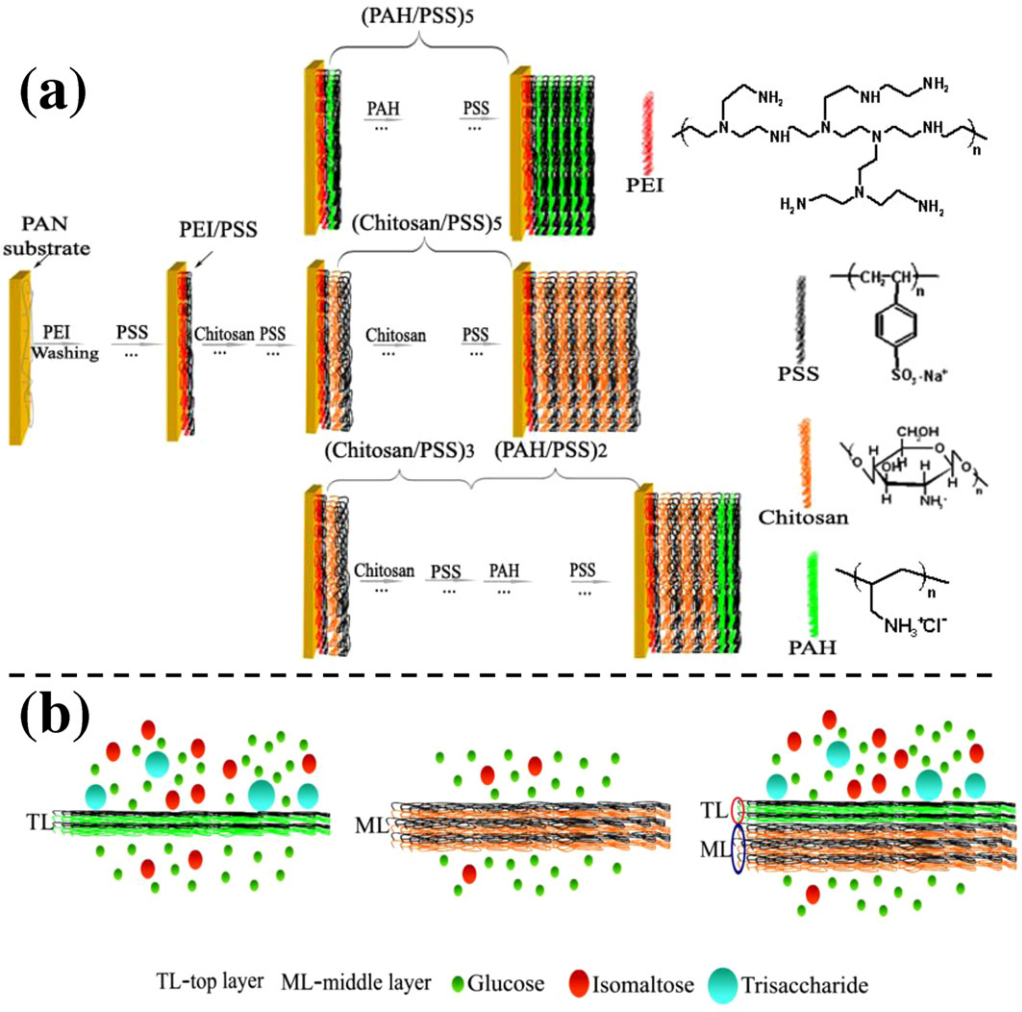

Fig. 1. (a) Preparation of $(PAH/PSS)_5$, $(chitosan/PSS)_5$ and C-PEM membranes and (b) the concentration profiles of glucose, maltose and oligosaccharides in the retention and permeation side of C-PEM membranes.

During the filtration process, the initial solution was stirred at high rate to diminish the concentration polarization. Permeated samples were collected in cooled flasks at certain period of time, measured and analyzed. The rejection ratio (R, %) was calculated by Eq. (2) upon the solute concentration of permeated and feed solution.

$$R = \left(1 - \frac{C_{perm}}{C_{feed}}\right) \times 100 \quad (2)$$

where C_{perm} was the solute concentration of permeated solution (gL^{-1}), while C_{feed} was the solute concentration of feed solution (gL^{-1}).

The selectivity (S) for solute A over solute B was defined by Eq. (3), which could be conveniently expressed in terms of rejection.

$$S = \frac{C_{A,perm}}{C_{A,feed}} \times \frac{C_{B,feed}}{C_{B,perm}} = \frac{100 - R_A}{100 - R_B} \quad (3)$$

where $C_{A,\ perm}$ or $C_{B,\ perm}$ was the solute A or B concentration of permeated solution (gL^{-1}), $C_{A,\ feed}$ or $C_{A,\ feed}$ was the solute A or B solution of feed solution (gL^{-1}), R_A or R_B was the rejection of solute A or B (%).

The permeation was stopped when the retention reached a constant value and then quantified using high performance liquid chromatography (HPLC) performed on an analytical column (Tsk-gel Amide 80, 5 μm, 4.6 mm id × 250 mm). The samples were diluted with acetonitrile prior to analysis. For the elution conditions, the mobile phase was 70% acetonitrile and 30% water. Temperature was kept constant at 50 °C, with a flow rate of 0.8 mL min^{-1} and an injection volume of 20 μL. The detection used a Knauer Differential-Refractometer. In each set of experiment, a standard curve was plotted with saccharide solution of different concentrations. All the measurements were based on at least three samples, and the average values were used. The standard deviation on the measurements was about 5%.

3. Results and discussion

3.1. Characterizations of the polyelectrolyte multilayer (PEM) membranes

3.1.1. SEM images

The cross-sectional images of the PAN and hydrolyzed PAN membranes are shown in Fig. S1. Loosely opened pores and finger-like pores could be observed for both of the membranes as shown in Fig. S1a and S1b. This indicated the porous support layer remained intact after hydrolysis. Additionally, the surface morphologies of the PEM membranes were also investigated as shown in Fig. S2. The PAN and hydrolyzed PAN membranes both exhibited smooth surface, while the PEM membranes showed rougher surface. Specifically, $(PAH/PSS)_5$ membranes displayed

much smoother surface than $(chitosan/PSS)_5$ membranes as illustrated in Fig. S2c and S2d, which might result in less fouling propensity (Al-Amoudi & Lovitt, 2007; Van der Bruggen, Mänttäri, & Nyström, 2008). As a result of the similar surface chemical component, C-PEM membranes demonstrated almost the same surface morphology with that of $(PAH/PSS)_5$ membranes (Fig. S2e).

3.1.2. AFM images

Previous work (Li et al., 2008; Li, Loo, Richard, & Green, 2005) reported that the PEMs usually possessed a nanoscale thickness. Herein, tapping mode AFM experiment was conducted to testify the thickness of the PEMs for C-PEM membranes. For measurement convenience, a sample was deposited on a negatively treated glass slide instead of a polymer support, followed by the same operational procedure. As shown in Fig. S3, the AFM image suggested that the thickness of the PEMs was about 24 nm. It was worth mentioning that, in order to reduce the differences of surface property between the hydrolyzed PAN membranes and glass slides, the $(PEI/PSS)_1$ bilayer was pre-assembled on both of the two substrates.

3.1.3. ATR-FTIR study of PEMs

ATR-FTIR spectra confirmed the LbL assembly of the chitosan/PSS and PAH/PSS multilayers on the hydrolyzed PAN membranes. Although large background absorbance from the hydrolyzed PAN membranes obscured several peaks, no absorbance in the region around 1190 cm^{-1} and 1033 cm^{-1} (Fig. 2a) could be found. As a result, these two peaks appeared in the PEM membranes should be attributed to the asymmetrical and symmetrical stretching vibration of S=O group. Moreover, the intensity of these two peaks enhanced with an increase of bilayer number, providing strong evidence that the adsorption amount of PSS grew linearly with an increase of bilayer number. This linearly increase for the PAH/PSS multilayers was in accordance with the previous work (Lavalle et al., 2002; Malaisamy & Bruening, 2005) that conducted by ellipsometry. Similarly, the FTIR spectra of the chitosan/PSS multilayers were also in accordance with the previous work (Aravind, Mathew, & Aravindakumar, 2007) with a linearly increased intensity of S=O as a function of layer number (Fig. 2b).

Through comparing the FTIR spectra of the multilayers for $(chitosan/PSS)_5$, $(PAH/PSS)_5$ and C-PEM membranes, similar intensity of the peaks at 1190 cm^{-1} and 1033 cm^{-1} (Fig. 2c) indicated that the same amounts of PSS were assembled for each membrane. As shown in Fig. 1a, the molecular structures revealed that both PAH and chitosan contained one positive charge in a monomer. Hence, identical moles of chitosan and PAH could be adsorbed to a negatively charged layer. Meanwhile, each fully protonated chitosan and PAH contained one positive charge per 11 and 4 non-hydrogen atoms. According to the previous result (Malaisamy & Bruening, 2005), the swelling property was related to the number of non-hydrogen atoms per polyelectrolyte monomer. It could be derived that the $(chitosan/PSS)_5$ multilayers would swell more than the $(PAH/PSS)_5$ multilayers, and result in a higher permeability (Ramsden, Lvov, & Decher, 1995; Wong, Rehfeldt, Hänni, Tanaka, & Klitzing, 2004).

To further monitor the assembly process of the PEMs for C-PEM membranes, the zeta potential of the PEMs as a function of layer number was carried out as shown in Fig. 2d. It could be found that the zeta potential of the PEMs totally located at the range of −6 mV–6 mV, revealing the interlay electrostatic interaction. This result further verified the successful alternative assembly of opposite charged polyelectrolytes.

3.2. NF process

3.2.1. NF properties for different types of the PEM membranes

To investigate the separation properties of the PEM membranes, NF process was performed by using IMO500 solution (10 gL^{-1}) as feed solution (The IMO500 concentration means the total weight content of IMO500 in the aqueous solution.). In any case, owing to the nearly complete rejection of oligosaccharides, separation of glucose and maltose became the key issue. Based on size-selective transport model (Liu & Bruening, 2004; Pontalier, Ismail, & Ghoul, 1997), the concentration profile of each saccharide in the retention and permeation side could be described as Fig. 1b.

Table 1 summarized the NF property of IMO500 solution for several PEM membranes. Compared to the rejection ($79.0 \pm 0.6\%$) of glucose performed by $(PAH/PSS)_5$ membranes, C-PEM membranes exhibited a relatively lower rejection ($63.0 \pm 0.5\%$) of glucose along with a higher maltose/glucose selectivity of 46. Moreover, in Table 1, it could be observed that majority of glucose could pass through $(chitosan/PSS)_3$ and $(chitosan/PSS)_5$ membranes, indicating that the ML of C-PEM membranes mainly contributed to enhance the permeability of glucose as compared with the TL. To further clarify the role of the ML and TL on the NF performance, C-PEM membranes with the reverse order of the TL and ML was fabricated and denoted as C-PEM^a membranes. Interestingly, this C-PEM^a membranes showed rather low permeation flux and complete rejection for all the saccharides as illustrated in Table 1. This phenomenon could be explained as follows: the chitosan chains penetrated into the TL because of their high mobility, enhancing the ionic-crosslinking degree between the TL and ML and finally resulting in smaller pore size (Miller & Bruening, 2005).

The results in the previous work (Park, Barrett, Rubner, & Mayes, 2001) indicated that the use of polyelectrolytes with higher charged density could induce stronger ionic-crosslinked PEM membranes, which would result in higher rejection of neutral molecules. The rejection for glucose, maltose and oligosaccharides decreased in the order of $(PAH/PSS)_5$ > C-PEM > $(chitosan/PSS)_5$, which could be also ascribed to the ordered charge density. For a single-paired polyelectrolyte membranes, $(chitosan/PSS)_5$ membranes exhibited higher permeation flux (7.3 ± 0.5 Lm^{-2} h^{-1}) than $(PAH/PSS)_5$ membranes (3.0 ± 0.2 Lm^{-2} h^{-1}) due to its higher swelling properties. To acquire higher permeability with moderate oligosaccharide separation property, the three PAH/PSS bilayers of $(PAH/PSS)_5$ membranes were replaced by $(chitosan/PSS)_3$ multilayers, which were then designated as the ML of C-PEM membranes to allow more solvent to pass through. Therefore, C-PEM membranes could acquire a permeation flux of 3.7 ± 0.3 Lm^{-2} h^{-1}, which was higher than that of $(PAH/PSS)_5$ membranes.

In addition, NF experiment was also carried out by using $(PAH/PSS)_3$ membranes. Compared to C-PEM membranes, slightly higher permeation flux (3.2 ± 0.3 Lm^{-2} h^{-1}) and lower retention ($60.0 \pm 0.2\%$ for glucose and $95.0 \pm 0.6\%$ for maltose) were acquired for $(PAH/PSS)_3$ membranes arising from the following facts: the $(chitosan/PSS)_2$ multilayers in C-PEM membranes were also able to reject lager molecules resulting in a higher selectivity of glucose/maltose; chitosan, as highly hydrophilic polymer, could form numerous water channels within the membranes resulting in little decrease of permeation flux.

3.2.2. Influence of the operation pressure on permeation flux and rejection for C-PEM membranes

Table 2 showed that the permeation flux of IMO500 solution (10 gL^{-1}) increased approximately linearly with the operation pressure. Meanwhile, pore size reduction caused by pressure-induced compaction also induced an increased rejection of each kind of saccharide. Specifically, higher pressure could increase the permeation flux of the solvent (water), but not the permeation flux of

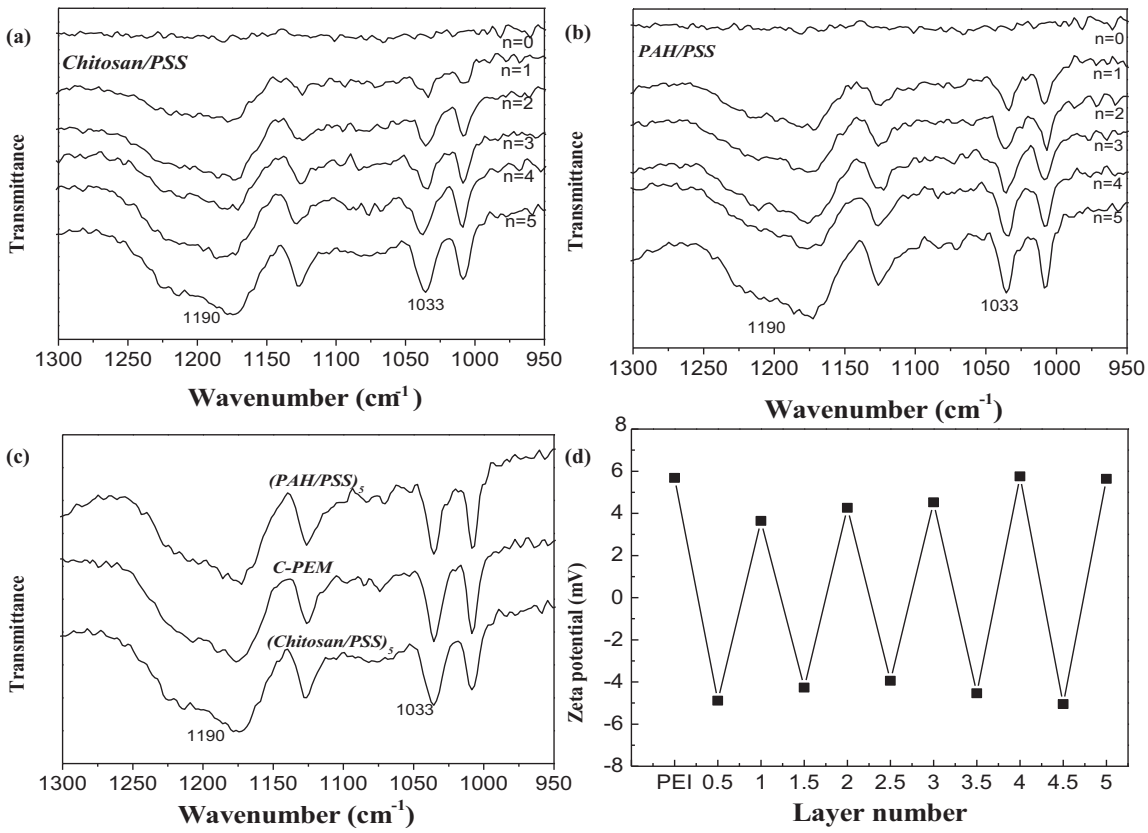

Fig. 2. ATR-FTIR spectra of (a) $(chitosan/PSS)_n$ and (b) $(PAH/PSS)_n$ multilayers as well as (c) $(PAH/PSS)_5$, C-PEM and $(chitosan/PSS)_5$ membranes; (d) surface zeta potential of C-PEM membranes as a function of layer number.

Table 1
Summary of nanofiltration performance of different types of membranes.

Types of membranes	Permeation flux (J) ($Lm^{-2}\,h^{-1}$)	Rejection (R), %			Maltose/glucose selectivity (S)
		Glucose	Maltose	Oligosaccharides	
$(Chitosan/PSS)_3$	9.2 ± 0.7	25.3 ± 0.4	72.1 ± 0.4	91.0 ± 0.5	2.6
$(Chitosan/PSS)_5$	7.3 ± 0.5	40.0 ± 0.3	90.0 ± 0.4	100	6
$(PAH/PSS)_3$	3.2 ± 0.3	60.0 ± 0.2	95.0 ± 0.6	100	8
$(PAH/PSS)_5$	3.0 ± 0.2	79.0 ± 0.6	99.5 ± 0.3	100	42
C-PEM	3.7 ± 0.3	63.0 ± 0.5	99.2 ± 0.3	100	46
C-PEM[a]	1.5 ± 0.2	100.0	100.0	100	–

C-PEM[a]: C-PEM with the reversed order of top layer and middle layer, that is, chitosan/PSS as top layer while PAH/PSS as the middle layer.

the solute (saccharides) due to their larger molecule size. The combination of higher water flux and constant solute flux resulted in higher saccharides rejection. It should be noted that the rejection of glucose seemed to increase more obviously than other larger-sized saccharides because of the rather high rejection of maltose and oligosaccharides.

Table 2
Effect of operation pressure on permeation flux and rejection for C-PEM membranes.

Operation pressure (MPa)	Permeation flux (J) ($Lm^{-2}\,h^{-1}$)	Rejection (R), %		
		Glucose	Maltose	Oligosaccharides
0.2	2.1 ± 0.3	49.0 ± 0.6	99.0 ± 0.3	100
0.3	3.7 ± 0.3	63.0 ± 0.5	99.2 ± 0.3	100
0.4	4.7 ± 0.2	70.0 ± 0.2	99.6 ± 0.4	100

3.2.3. *Influence of the IMO500 concentration on permeation flux and rejection for C-PEM membranes*

As was well known, concentration polarization, solution viscosity and osmotic pressure would all increase with the increase of the IMO500 concentration, which exerted a remarkable effect on the permeation flux and rejection as shown in Table 3. In detail, the rejection of IMO500 components especially glucose decreased as the total concentration increased, which was in accordance with the results of previous report (Li et al., 2004). This could be explained as follows: (1) the thickness and viscosity of the concentration polarization layer increased with the increase of oligosaccharides concentration, resulting in more amount of glucose passing through the membranes; (2) the rejection of maltose and oligosaccharides changed little because of their rather high rejection (>99%) at the concentration ranging from 5–30 gL^{-1}.

Table 3
Effect of IMO500 concentration on permeation flux and rejection for C-PEM membranes.

Concentration (gL^{-1})	Viscosity (cP)	Permeation flux (J) ($Lm^{-2}\,h^{-1}$)	Rejection (R), %		
			Glucose	Maltose	Oligosaccharides
5	3.00	5.0 ± 0.4	65.0 ± 0.3	99.6 ± 0.3	100
10	3.18	3.7 ± 0.3	63.0 ± 0.5	99.2 ± 0.3	100
20	3.30	2.6 ± 0.3	58.0 ± 0.6	99.0 ± 0.5	100
30	3.42	2.1 ± 0.2	50.0 ± 0.6	98.8 ± 0.4	100

3.2.4. Influence of stirring rate on permeation flux and rejection for C-PEM membranes

Near-surface stirring was also proved to influence the NF separation property. In the present study, a set of stirring rate N (0, 100, 200, 300, 400 rpm, respectively) was applied in the filtration process. Accordingly, the Reynold number (Re) values were about 2.9×10^4, 5.8×10^4, 8.7×10^4 and 11.6×10^4, respectively, which were fallen into the turbulent flow region. The average shear rates, estimated based on the typical empirical assumption that the feed solution was Newtonian fluid, (Sánchez Pérez, Rodríguez Porcel, Casas López, Fernández Sevilla, & Chisti, 2006) were about 10.2, 29.0, 53.2 and 83.7 s^{-1}. As reported in previous literature (Ng & Elimelech, 2004; Vogel et al., 2010), lower average shear rate would accelerate the growth of the cake layer at the membrane surface, which would result in cake-enhanced concentration polarization effect. On one hand, the cake-enhanced concentration polarization, which meant a kind of membrane fouling, would lead to a decrease of solution permeation flux. As shown in Fig. 3, the permeation flux reduced from 3.7 ± 0.3 to 1.5 ± 0.1 $Lm^{-2}\,h^{-1}$ as the stirring rate lowered from 400 to 0 rpm (corresponding to the average shear rate γ = 83.7 to 0 s^{-1}). On the other hand, the cake-enhanced concentration polarization would lead to a higher concentration of solute at the membrane surface. Since the intrinsic retention of the membrane was unchanged, the cake-enhanced concentration polarization could eventually result in a higher solute concentration in the permeate, that was, a decrease in retention. From the evaluation of the membrane separation performance for the IMO500 solution, it could be found the rejection of each saccharide reduced with the decrease of stirring rate from 400 to 0 rpm. In particular, the rejection of glucose significantly decreased from 63.9 to 50.5%.

3.2.5. Influence of pH values of the feed solution on permeation flux for C-PEM membranes

Since the degree of ionization of C-PEM membranes was pH sensitive, it was possible to tune the NF properties of the membranes by switching pH values. In this study, the permeation flux as a function of pH values of the IMO500 solution was investigated. The operation pressure was fixed at 0.3 MPa and IMO500 concentration in the feed solution was 10 gL^{-1}.

According to C. Déjugnat's research (Glinel et al., 2007), weak polyelectrolytes like PAH and chitosan could be affected by pH values more drastically than strong polyelectrolyte like PSS. Under basic condition (usually the pH value was above 9), the–NH_3^+ groups within chitosan and PAH molecules partially converted into–NH_2 groups, which considerably reduced the interaction between polycation (chitosan and PAH) and PSS (Deng et al., 2008; Mauser, Déjugnat, & Sukhorukov, 2004; Zhang & Gonsalves, 1998). Additionally, most amount of the negative charge was left to cause the increase of the repulsive force, resulting in the enlargement of membrane pore size and the subsequent delamination of PEMs. Accordingly, as shown in Fig. 4, a drastic flux increase was found when the pH value was switched from neutral (3.7 $Lm^{-2}\,h^{-1}$) to basic (7.6 $Lm^{-2}\,h^{-1}$) condition.

Under acid or neutral pH conditions, the interaction among these polyelectrolytes kept strong to prevent the detachment of PEMs from the support layer. Accordingly, similar permeation flux (3.7 $Lm^{-2}\,h^{-1}$) could be found under acid or neutral pH conditions.

3.2.6. Stability test of C-PEM membranes

An experiment over an extended period (about 48 h) was implemented using C-PEM membranes for the separation of the IMO500 solution. The results in Fig. 5 indicated that C-PEM membranes displayed stable permeability and retention performance. Specifically, with the prolongation of operation time from 0 to 48 h, the permeation flux showed only a slight increase from 3.70 to 3.81 $Lm^{-2}\,h^{-1}$. Meanwhile, negligible change or even a bit increase in the rejection of each saccharide was found. This phenomenon could be explained as follows: the leaching of trace polyelectrolytes took place during the long-term stirring, rendering C-PEM membranes a bit larger pore size which still lied between molecular size of water and saccharides, consequently, allowing more water molecules to pass

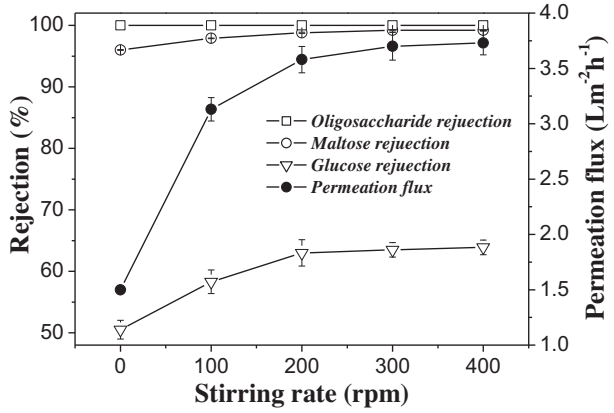

Fig. 3. Influence of stirring rate on permeation flux and rejection of C-PEM membranes.

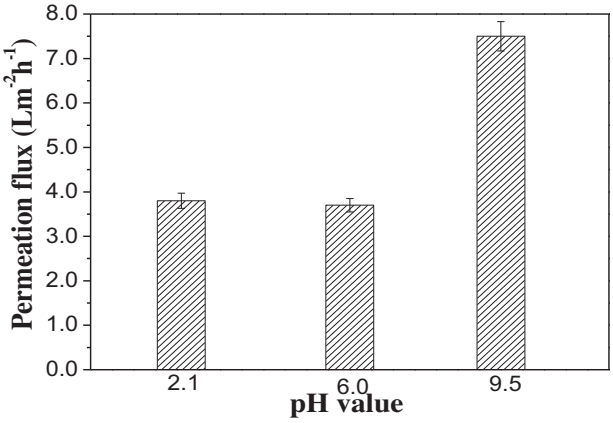

Fig. 4. Influence of pH value on permeation flux of C-PEM membranes.

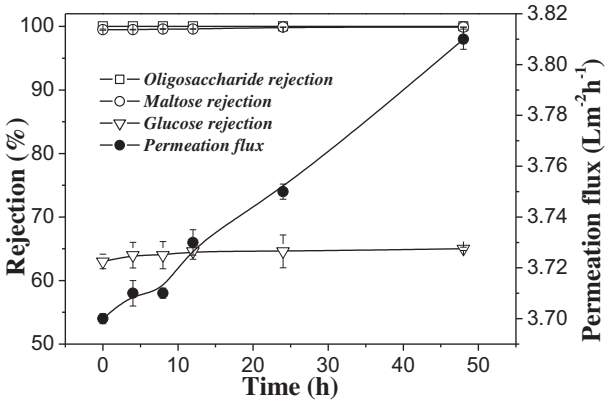

Fig. 5. Short-term stability test of C-PEM membranes for IMO500 purification.

through without significantly changing the rejection of oligosaccharides.

4. Conclusions

In summary, composite polyelectrolyte multilayer (C-PEM) membranes have been fabricated *via* layer-by-layer assembly technique for oligosaccharides nanofiltration separation. The $(chitosan/PSS)_3$ multilayers (the middle layer, ML) were assembled on the hydrolyzed polyacrylonitrile (PAN) ultrafiltration membranes, while the $(PAH/PSS)_2$ multilayers (the top layer, TL) were assembled on the ML to form C-PEM membranes. Characterizations including SEM, AFM, FTIR and zeta potentials have confirmed the successful formation of C-PEM membranes. During nanofiltration separation of oligosaccharides, C-PEM membranes exhibited enhanced selectivity and moderate permeation flux compared with single-paired PEM membranes such as $(PAH/PSS)_5$ membranes or $(chitosan/PSS)_5$ membranes. Specifically, C-PEM membranes acquired high rejection of maltose ($99.2 \pm 0.3\%$) and oligosaccharides (100%), relatively low rejection of glucose ($63.0 \pm 0.5\%$), and high selectivity of 46 for maltose/glucose. Meanwhile, the separation performance of C-PEM membranes could be tuned by several operation parameters, such as feed concentration, operation pressure, stirring rate or pH value. Hopefully, the desirable and controllable performance would render C-PEM membranes potentially attractive for practical oligosaccharides purification.

Acknowledgments

The authors thank the financial support from the National Basic Research Program of China (2009CB724705), National Science Fund for Distinguished Young Scholars (21125627), the National Science Foundation of China (20976127), and the Program of Introducing Talents of Discipline to Universities (B06006).

Appendix A. Supplementary data

Supplementary data associated with this article can be found, in the online version, at http://dx.doi.org/10.1016/j.carbpol.2013.01.044.

References

Ahmadiannaminia, P., Li, X. F., Goyensa, W., Joseph, N., Meesschaert, B., & Vankelecom, I. F. J. (2012). Multilayered polyelectrolyte complex based solvent resistant nanofiltration membranes prepared from weak polyacids. *Journal of Membrane Science*, *394–395*, 98–106.

Al-Amoudi, A., & Lovitt, R. W. (2007). Fouling strategies and the cleaning system of NF membranes and factors affecting cleaning efficiency. *Journal of Membrane Science*, *303*, 4–28.

Anderson, J. W., & Hanna, T. J. (1999). Impact of nondigestible carbohydrates on serum lipoproteins and risk for cardiovascular disease. *The Journal of Nutrition*, *129*, 1457S–1466S.

Aravind, U. K., Mathew, J., & Aravindakumar, C. (2007). Transport studies of BSA, lysozyme and ovalbumin through chitosan/polystyrene sulfonate multilayer membrane. *Journal of Membrane Science*, *299*, 146–155.

Beppu, M., Vieira, R., Aimoli, C., & Santana, C. (2007). Crosslinking of chitosan membranes using glutaraldehyde: Effect on ion permeability and water absorption. *Journal of Membrane Science*, *301*, 126–130.

Chen, P. H., Kuo, T. Y., Liu, F. H., Hwang, Y. H., Ho, M. H., Wang, D. M., et al. (2008). Use of dicarboxylic acids to improve and diversify the material properties of porous chitosan membranes. *Journal of Agricultural and Food Chemistry*, *56*, 9015–9021.

De Oliveira, H., Fonseca, J., & Pereira, M. (2008). Chitosan-poly (acrylic acid) polyelectrolyte complex membranes: Preparation, characterization and permeability studies. *Journal of Biomaterials Science, Polymer Edition*, *19*, 143–160.

Deng, H. Y., Xu, Y. Y., Zhu, B. K., Wei, X. Z., Liu, F., & Cui, Z. Y. (2008). Polyelectrolyte membranes prepared by dynamic self-assembly of poly (4-styrenesulfonic acid-co-maleic acid) sodium salt (PSSMA) for nanofiltration (I). *Journal of Membrane Science*, *323*, 125–133.

Feng, Y., Chang, X., Wang, W., & Ma, R. (2009). Separation of galacto-oligosaccharides mixture by nanofiltration. *Journal of the Taiwan Institute of Chemical Engineers*, *40*, 326–332.

Glinel, K., Déjugnat, C., Prevot, M., Schöler, B., Schönhoff, M., & Klitzing, R. (2007). Responsive polyelectrolyte multilayers. *Colloids and Surfaces A: Physicochemical and Engineering Aspects*, *303*, 3–13.

Goulas, A. K., Grandison, A. S., & Rastall, R. A. (2003). Fractionation of oligosaccharides by nanofiltration. *Journal of the Science of Food and Agriculture*, *83*, 675–680.

Jin, W., Toutianoush, A., & Tieke, B. (2003). Use of polyelectrolyte layer-by-layer assemblies as nanofiltration and reverse osmosis membranes. *Langmuir*, *19*, 2550–2553.

Kamada, T., Nakajima, M., Nabetani, H., Saglam, N., & Iwamoto, S. (2002). Availability of membrane technology for purifying and concentrating oligosaccharides. *European Food Research and Technology*, *214*, 435–440.

Lavalle, P., Gergely, C., Cuisinier, F., Decher, G., Schaaf, P., Voegel, J., et al. (2002). Comparison of the structure of polyelectrolyte multilayer films exhibiting a linear and an exponential growth regime: An in situ atomic force microscopy study. *Macromolecules*, *35*, 4458–4465.

Li, W., Li, J., Chen, T., & Chen, C. (2004). Study on nanofiltration for purifying fructo-oligosaccharides: I. Operation modes. *Journal of Membrane Science*, *245*, 123–129.

Li, X., De Feyter, S., Chen, D., Aldea, S., Vandezande, P., Du Prez, F., et al. (2008). Solvent-resistant nanofiltration membranes based on multilayered polyelectrolyte complexes. *Chemistry of Materials*, *20*, 3876–3883.

Li, Y., Loo, Y. L., Richard, A., & Green, P. F. (2005). Influence of interfacial constraints on the morphology of asymmetric crystalline-amorphous diblock copolymer films. *Macromolecules*, *38*, 7745–7753.

Liu, X., & Bruening, M. L. (2004). Size-selective transport of uncharged solutes through multilayer polyelectrolyte membranes. *Chemistry of Materials*, *16*, 351–357.

López-Leiva, M. H., & Guzman, M. (1995). Formation of oligosaccharides during enzymic hydrolysis of milk whey permeates. *Process Biochemistry*, *30*, 757–762.

Malaisamy, R., & Bruening, M. L. (2005). High-flux nanofiltration membranes prepared by adsorption of multilayer polyelectrolyte membranes on polymeric supports. *Langmuir*, *21*, 10587–10592.

Mauser, T., Déjugnat, C., & Sukhorukov, G. B. (2004). Reversible pH-dependent properties of multilayer microcapsules made of weak polyelectrolytes. *Macromolecular Rapid Communications*, *25*, 1781–1785.

Miller, M. D., & Bruening, M. L. (2004). Controlling the nanofiltration properties of multilayer polyelectrolyte membranes through variation of film composition. *Langmuir*, *20*, 11545–11551.

Miller, M. D., & Bruening, M. L. (2005). Correlation of the swelling and permeability of polyelectrolyte multilayer films. *Chemistry of Materials*, *17*, 5375–5381.

Mussatto, S. I., & Mancilha, I. M. (2007). Non-digestible oligosaccharides: A review. *Carbohydrate Polymers*, *68*, 587–597.

Ng, H. Y., & Elimelech, M. (2004). Influence of colloidal fouling on rejection of trace organic contaminants by reverse osmosis. *Journal of Membrane Science*, *244*, 215–226.

Park, S. Y., Barrett, C. J., Rubner, M. F., & Mayes, A. M. (2001). Anomalous adsorption of polyelectrolyte layers. *Macromolecules*, *34*, 3384–3388.

Pontalier, P. Y., Ismail, A., & Ghoul, M. (1997). Mechanisms for the selective rejection of solutes in nanofiltration membranes. *Separation and Purification Technology*, *12*, 175–181.

Ramsden, J., Lvov, Y. M., & Decher, G. (1995). Determination of optical constants of molecular films assembled via alternate polyion adsorption. *Thin Solid Films*, *254*, 246–251.

Richert, L., Lavalle, P., Payan, E., Shu, X. Z., Prestwich, G. D., Stoltz, J. F., et al. (2004). Layer by layer buildup of polysaccharide films: Physical chemistry and cellular adhesion aspects. *Langmuir*, *20*, 448–458.

Roberfroid, M. B. (1999). Concepts in functional foods: The case of inulin and oligofructose. *Journal of Nutrition*, *129*, 1398S–1401S.

Sánchez Pérez, J. A., Rodríguez Porcel, E. M., Casas López, J. L., Fernández Sevilla, J. M., & Chisti, Y. (2006). Shear rate in stirred tank and bubble column bioreactors. *Chemical Engineering Journal*, *124*, 1–5.

Stanton, B. W., Harris, J. J., Miller, M. D., & Bruening, M. L. (2003). Ultrathin, multilayered polyelectrolyte films as nanofiltration membranes. *Langmuir*, *19*, 7038–7042.

Van der Bruggen, B., Mänttäri, M., & Nyström, M. (2008). Drawbacks of applying nanofiltration and how to avoid them: A review. *Separation and Purification Technology*, *63*, 251–263.

Vogel, D., Simon, A., Alturki, A. A., Bilitewski, B., Price, W. E., & Nghiem, L. E. (2010). Effects of fouling and scaling on the retention of trace organic contaminants by a nanofiltration membrane: The role of cake-enhanced concentration polarisation. *Separation and Purification Technology*, *73*, 256–263.

Wang, J., Yao, Y., Yue, Z., & Economy, J. (2009). Preparation of polyelectrolyte multilayer films consisting of sulfonated poly (ether ether ketone) alternating with selected anionic layers. *Journal of Membrane Science*, *337*, 200–207.

Wong, J. E., Rehfeldt, F., Hänni, P., Tanaka, M., & Klitzing, R. v. (2004). Swelling behavior of polyelectrolyte multilayers in saturated water vapor. *Macromolecules*, *37*, 728–7289.

Xu, Q., Chao, Y. L., & Wan, Q. B. (2009). Health benefit application of functional oligosaccharides. *Carbohydrate Polymers*, *77*, 435–441.

Zhang, S., & Gonsalves, K. E. (1998). Influence of the chitosan surface profile on the nucleation and growth of calcium carbonate films. *Langmuir*, *14*, 6761–6766.

Zhao, H. F., Hua, X., Yang, R. J., Zhao, L. M., Zhao, W., & Zhang, Z. (2012). Diafiltration process on xylo-oligosaccharides syrup using nanofiltration and its modelling. *International Journal of Food Science & Technology*, *47*, 32–39.